

Determination of the latest sediment accumulation rates and pattern by performing ^{210}Pb models and ^{137}Cs technique in the Lake Bafa, Mugla, Turkey

I. Sert¹ · F. E. Ozel² · G. Yaprak¹ · M. Eftelioglu²

Received: 12 January 2015 / Published online: 20 June 2015
© Akadémiai Kiadó, Budapest, Hungary 2015

Abstract The sediment chronology was determined using Lead-210 (^{210}Pb) and Cesium-137 (^{137}Cs) dating method. Profile distributions of Polonium-210 (^{210}Po) and ^{210}Pb were evaluated with regarding to sediment porosity, core location, bottom currents and prevalent winds. Max. ^{210}Po and ^{210}Pb activity concentrations are found as 193.83 ± 4.43 and 187.84 ± 4.84 Bq kg⁻¹ respectively. According to vertical radionuclide ($^{210}\text{Po}/^{210}\text{Pb}$) ratios, sediments especially in east part of the lake are rich with respect to the fecal pellets. Residence time of the ^{210}Pb is calculated as 1.9 months in the lake. Average sedimentation rate (0.359 ± 0.012 cm year⁻¹) in central area is higher than the near shore (0.137 ± 0.006 cm year⁻¹) one in Lake Bafa.

Keywords Sedimentation rate · Fecal pellets · Residence time of the ^{210}Pb · Natural (^{210}Po , ^{210}Pb) · Artificial (^{137}Cs) radionuclides

Introduction

Lake Bafa is a natural reserve situated in southwestern ($37^{\circ}31'\text{N}$, $27^{\circ}27'\text{E}$) Turkey, the southern part of it within the boundaries of Milas district of Mugla Province and

the northern part within Aydin Province's Soke district. It is one of the largest coastal lakes in Turkey. Having a maximum depth of roughly 20 m, its surface covers an area of approximate 75 km². The lake developed as a result of the delta progradation of the Buyuk Menderes (Meander) River which is the longest river in the Aegean region Menderes for 584 km through western part of Turkey before reaching the Aegean Sea with a large delta ecosystem. Buyuk Menderes has a total drainage area of 24,000 km². The overall runoff capacity, for instances the erosion potential of the river is so high that, it could be able to change the geomorphology of the former Latmian Bay radically [1]. In the past six or so millennia, the river sediments have gradually filled nearly the whole marine embayment of the so-called Latmian Gulf, thereby separating its southeastern part from the off shore [2]. Lake Catchment is comprised of the residential and agricultural areas and there is also olive oil factory, fish hatchery, restaurant in catchment in Fig. 1. showing that it has been affected by the human activities. The industry has been gradually grown in catchment land in recent years. Lake is under the influence of waters runoff coming from the Buyuk Menderes River. Beside this, some small streams contribute to the water input [1]. Salinity of the lake water differs in a range between 0.17 and 0.04 % [3], summer and winter seasons respectively.

The radionuclides ^{210}Po (half-life: 138.38 days), ^{210}Pb (half-life: 22.30 years) and ^{137}Cs (half-life: 30.14 years) have widely and successfully used in environmental investigations. In this study radiometric measurements are shedded light on evaluation of lake sediments, especially recent chronology, residence time of ^{210}Pb , radionuclide ratios, pollution degree and supply of pollution.

✉ I. Sert
ilker.sert@ege.edu.tr

¹ Institute of Nuclear Sciences, Ege University, Bornova, 35100 Izmir, Turkey

² Institute of Marine Sciences and Technology, Dokuz Eylul University, Inciralti, 35340 Izmir, Turkey



Fig. 1 Study area and core locations

Materials and methods

Sample preparation and measurement

Four sediment cores (C-1, C-2, C-3 and C-4) were collected from different locations of Lake Bafa via a gravity corer in 2010. Study area is shown in Fig. 1. Bottom currents were measured in each station at different depths (6, 8, 10, 12 m) by using Teledyne 150 kHz RDI WH Mariner ADCP (Acoustic Doppler Current Profiler). The core length is varied from 32 to 51 cm and water depth is from 3 to 17 m. Cores were sliced at 1 cm intervals in the laboratory. The wet weights of the samples were recorded and then oven dried at 70 °C for 24 h to obtain dry weights. Then water content and porosity were calculated for each slice.

The sediment samples were ground and passed through a 63 μm mesh followed by homogenization. After the addition of a standardized amount of ^{209}Po (half-life: 103 years) tracer, sediment samples were completely dissolved with $\text{HF}:\text{HNO}_3$ (1:1) and HCl . Polonium was spontaneously plated onto copper discs in 0.5 M HCl in the presence of ascorbic acid to reduce Fe^{+3} to Fe^{+2} in order to get the optimum conditions for plating ^{210}Po on discs the standard technique used which was modified by Flynn [4]. Measurements of ^{210}Po concentrations were made through its 5.30 MeV alpha particle emission, using ^{209}Po (4.88 MeV alpha emission) as the internal tracer (National Institute of Standards and Technology, <500 Bq in 7 % hydrochloric acid). Alpha particles from ^{210}Po were

counted in PIPS (Passivated Implanted Planar Silicon) detector (Ortec Octete Plus-450 mm^2 ULTRA-AS) and analyzed by utilizing a Canberra 7401 spectrometer. After the first deposition of ^{210}Po residual 0.5 M HCl was stored for one year to allow of ^{210}Po in-growth from the ^{210}Pb contained in the sample solution. Each sample was re-plated to determine the ^{210}Po activity. Counting period was adjusted to keep the standard error under the 10 % (relative standard error was approximately 5 %). In determination of ^{210}Po , the results of ^{209}Po recovery and Bateman equations [5, 6] were used.

^{137}Cs activities were determined as gamma spectroscopic using the high resolution gamma spectrometer consist of a 184 cc HPGe detector, ORTEC-671 model spectroscopy amplifier and a Canberra PC based multi-channel analyzer with a 8 K spectral memory. The specification of the p-type coaxial detector was 1.85 keV full width at half maximum (FWHM) at the 1.33 MeV gamma energy of ^{60}Co and a 25 % relative efficiency. Minimum detectable activity (MDA) was 2.21 Bq kg^{-1} for 200000 s. To reduce the background, the detector was shielded by a 100 mm thick lead shield with a fixed bottom and a moving cover. The detector efficiency calibration was performed by using the IAEA quality assurance reference materials produced by IAEA [7]. Sample was comprised of 10 g sediment and 4 g starch (Merck). Geometry was formed by using presser as a disc (thickness was 6 mm and diameter was 40 mm). Reference material with same geometry was IAEA-156.

Residence time calculation

Residence time of ^{210}Pb in lake water was calculated using the first order kinetic relation as shown below:

$$dI_w/dt = \Phi_w - \{[\lambda_{pb} + (1/T_w)]I_w\} \tag{1}$$

$$dI_s/dt = \Phi_s - \{[\lambda_{pb} + (1/T_s)]I_s\} \tag{2}$$

where Φ_w and Φ_s ($\text{Bq cm}^{-2} \text{ year}^{-1}$) are the fluxes of ^{210}Pb in the lake water and sediments respectively, and their corresponding inventories I_w and I_s (Bq cm^{-2}). λ_{pb} is the radioactive decay constant ($= \ln 2/22.3 \text{ year}^{-1}$), T_w and T_s are the residence times of the ^{210}Pb in the lake water and lake sediments respectively. At steady state, the inventory of unsupported ^{210}Pb in the lake water, I_w , can be found by subtraction the mean sedimentary unsupported ^{210}Pb inventory of the lake, I_s from the atmospherically supported inventory, I_{atm} . If dI_w and dI_s/dt are equal to zero residence time of ^{210}Pb in lake water can be obtained using above equations as:

$$T_w \approx \frac{I_{atm} - I_s}{\lambda_{pb} I_s} \tag{3}$$

Since $\lambda_{pb} \ll 1/T_w$, $\lambda_{pb} \ll 1/T_s$ and $I_w = I_a - I_s$ [8].

Results and discussions

Nevertheless there is not any study of sedimentation rates and historical sediment records in Lake Bafa using such models at present. In this study, we have examined the applicability of the ^{210}Pb dating models for determination of past sedimentation rates in Lake Bafa in Turkey. The use of ^{210}Pb dating models was tested with ^{137}Cs dating. We have not only aimed to comprise out sedimentation pattern but also realized the works that are mentioned following sentences. $^{210}\text{Po}/^{210}\text{Pb}$ rates and porosities were determined in cores and consequences were used in evaluation of sediment content and supply of pollution. The residences time of ^{210}Pb in lake water were calculated In this research the most important point is that above mentioned evaluations for instances dating, sedimentation pattern, the residences time of radionuclide (^{210}Pb) and determination of sediment pollution degree ($^{210}\text{Po}/^{210}\text{Pb}$ rates) were especially realized by only using radiometric measurements.

Porosity

The porosity profile indicates that sediment structure in C-4 station consist of three types divisions with have different mass densities. Porosity is lower than the other three cores (Fig. 2).

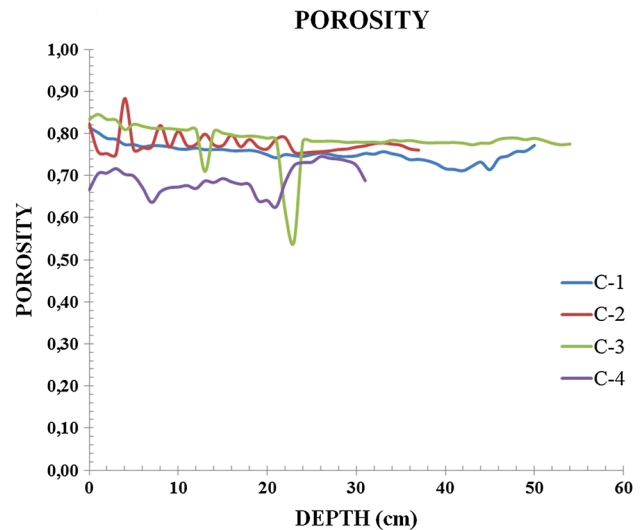


Fig. 2 Porosities of the sediment cores at C-1, C-2, C-3 and C-4 stations

Porosity displays more or less same value along the core profile. According to us it can be said that sediment structure which is accumulated to the lake floor is the same material along the core profile in C-3 station. When we compare porosity with the profile distribution of ^{210}Pb concentration, it is seen that sharply decrease in porosity corresponds to decrease in ^{210}Pb concentration (Table 1) and increase in sedimentation rate (Tables 2, 3).

C-2 station has successive increase and decrease in porosity and the values are relatively equal to each other. According to us it implies that sediment structure which is accumulated to the lake floor has been changed periodically and it is related to the Menderes River that its flow to the lake has periodically been banned for the irrigation. Beside of this it may be related to the collapse of the successive accumulated sediment layers and mixing them.

When examining the C-1 station it is seen that porosity along to core profile is more or less the same. In each core, porosities are free from the others due to the lack of bottom current in the lake. Measured flows were recorded between 3.046 and 4.905 cm s^{-1} . Speed of the bottom currents is very low. According to us, it has not any impression on sediment accumulation. Differences of the sedimentation rates among the stations are free from the bottom currents. So it can be stated as the lake has different sediment depositional zones.

Athy [9] argue that the porosity profile for homogeneous sediments with uniform compaction usually shows an exponential decrease with depth (obtained from [8]). Similarly Begy et al. [10] investigated that porosity profile shows an exponential decrease with depth in Red Lake (Romania). Contrary Klump et al. [11] calculated the fifteen porosity profiles, when glimpsed to the profiles they

Table 1 ^{210}Po , ^{210}Pb concentrations and $^{210}\text{Po}/^{210}\text{Pb}$ ratios are summarized in table

Depth (cm)	C-1			C-2			C-3			C-4		
	^{210}Po	^{210}Pb	$^{210}\text{Po}/^{210}\text{Pb}$	^{210}Po	^{210}Pb	$^{210}\text{Po}/^{210}\text{Pb}$	^{210}Po	^{210}Pb	$^{210}\text{Po}/^{210}\text{Pb}$	^{210}Po	^{210}Pb	$^{210}\text{Po}/^{210}\text{Pb}$
1	265.29	170.74	1.55	65.68	44.81	1.47	170.74	187.84	0.91	167.30	126.34	1.32
2	148.22	133.93	1.11	50.03	46.56	1.07	228.04	166.67	1.37	167.85	113.80	1.47
3	137.63	141.10	0.98	58.77	53.13	1.11	179.68	168.75	1.06	168.39	104.65	1.61
4	115.52	100.57	1.15	49.53	47.61	1.04	115.20	120.00	0.96	207.31	91.04	2.28
5	99.01	111.58	0.89	46.58	50.28	0.93	144.53	118.23	1.22	146.66	113.27	1.29
6	130.40	125.45	1.04	49.47	50.81	0.97	121.03	102.33	1.18	172.65	107.97	1.60
7	116.79	72.95	1.60	45.46	55.15	0.82	126.76	109.70	1.16	176.59	85.66	2.06
8	103.71	90.66	1.14	57.03	36.06	1.58	125.04	100.26	1.25	164.71	87.19	1.89
9	123.62	83.80	1.48	24.46	32.17	0.76	90.26	99.79	0.90	141.94	90.28	1.57
10	117.13	85.14	1.38	39.03	64.10	0.61	109.13	97.62	1.12	161.10	88.17	1.83
11	67.68	87.34	0.77	58.01	44.99	1.29	102.56	91.69	1.12	145.30	90.34	1.61
12	75.62	89.03	0.85	57.62	47.13	1.22	86.24	94.44	0.91	122.50	95.65	1.28
13	61.05	80.24	0.76	59.92	41.26	1.45	99.82	79.03	1.26	129.09	84.86	1.52
14	59.67	76.96	0.78	58.25	47.49	1.23	92.55	70.94	1.30	120.13	75.29	1.60
15	103.46	79.71	1.30	47.37	49.46	0.96	85.40	86.20	0.99	91.62	74.92	1.22
16	69.59	54.47	1.28	75.13	26.98	2.78	77.78	70.30	1.11	108.97	69.35	1.57
17	85.82	55.48	1.55	49.82	43.72	1.14	69.14	66.16	1.04	95.74	69.87	1.37
18	61.52	79.73	0.77	55.03	39.48	1.39	74.81	76.85	0.97	90.99	60.58	1.50
19	56.64	64.45	0.88	58.27	45.51	1.28	92.87	68.64	1.35	105.86	71.83	1.47
20	88.19	63.48	1.39	43.53	52.75	0.83	89.73	58.78	1.53	113.82	69.95	1.63
21	62.84	54.82	1.15	53.41	40.79	1.31	78.67	61.35	1.28	86.84	60.86	1.43
22	57.95	47.25	1.23	61.02	44.97	1.36	73.59	71.73	1.03	93.36	68.21	1.37
23	57.40	50.80	1.13	53.70	36.47	1.47	73.18	60.13	1.22	98.05	70.94	1.38
24	82.26	67.01	1.23	54.94	57.10	0.96	64.93	67.68	0.96	123.87	69.55	1.78
25	68.46	67.69	1.01	52.67	52.60	1.00	71.27	53.50	1.33	90.41	70.12	1.29
26	67.08	62.21	1.08	41.67	51.01	0.82	57.95	58.46	0.99	119.18	67.99	1.75
27	75.63	55.17	1.37	49.37	61.91	0.80	60.31	57.75	1.04	97.11	69.98	1.39
28	67.86	62.23	1.09	46.86	43.21	1.08	59.79	63.37	0.94	127.23	72.09	1.76
29	64.29	59.95	1.07	63.23	48.62	1.30	63.88	68.92	0.93	140.11	73.58	1.90
30	74.01	59.75	1.24	56.70	49.55	1.14	61.71	54.90	1.12	108.52	68.88	1.58
31	61.93	65.69	0.94	49.29	53.96	0.91	64.81	52.13	1.24	97.53	71.12	1.37
32	58.29	65.48	0.89	48.44	42.12	1.15	52.34	61.75	0.85	125.15	73.54	1.70
33	63.10	70.21	0.90			1.16	61.21	65.12	0.94			
34	57.66	60.58	0.95			1.02	69.84	54.07	1.29			
35	71.29	53.82	1.32			0.75	73.90	64.23	1.15			
36	63.25	69.87	0.91			1.15	29.97	68.21	0.44			
37	58.54	58.55	1.00			1.30	46.63	52.50	0.89			
38	41.96	60.21	0.70				67.64	59.94	1.13			
39	67.76	42.02	1.61				52.34	60.86	0.86			
40	59.68	55.54	1.07				60.98	61.09	1.00			
41	55.08	56.82	0.97				60.44	60.77	0.99			
42	62.93	51.65	1.22				89.04	55.56	1.60			
43	64.29	47.86	1.34				69.27	62.85	1.10			
44	64.05	57.44	1.12				50.70	52.81	0.96			
45	53.47	58.05	0.92				78.12	58.14	1.34			
46	71.25	59.04	1.21				66.84	63.57	1.05			
47	67.78	53.48	1.27				64.13	54.90	1.17			

Table 1 continued

Depth (cm)	C-1			C-2			C-3			C-4		
	²¹⁰ Po	²¹⁰ Pb	²¹⁰ Po/ ²¹⁰ Pb	²¹⁰ Po	²¹⁰ Pb	²¹⁰ Po/ ²¹⁰ Pb	²¹⁰ Po	²¹⁰ Pb	²¹⁰ Po/ ²¹⁰ Pb	²¹⁰ Po	²¹⁰ Pb	²¹⁰ Po/ ²¹⁰ Pb
48	79.37	49.34	1.61				56.32	62.17	0.91			
49	52.23	49.13	1.06				55.59	49.30	1.13			
50	69.70	56.66	1.23				47.12	49.08	0.96			
51	37.05	51.62	0.72				66.19	51.31	1.29			
52							57.37	59.76	0.96			
Average			1.12			1.15			1.09			1.58

Units of the concentrations are in mBq g⁻¹

Table 2 Sedimentation rates and dating in cores C-1, C-3, C-4 using CIC model

Depth (cm)	C-1			C-3			C-4		
	SR (cm year ⁻¹)	Dating (year)		SR (cm year ⁻¹)	Dating (year)		SR (cm year ⁻¹)	Dating (year)	
1	0.185	±0.007	2004.60 ±0.22	0.198	±0.005	2004.96 ±0.13	0.172	±0.005	2004.20 ±0.17
2	0.233	±0.010	2000.32 ±0.40	0.203	±0.006	2000.03 ±0.28	0.191	±0.006	1998.97 ±0.37
3	0.184	±0.006	1994.89 ±0.53	0.168	±0.005	1994.10 ±0.43	0.213	±0.006	1994.27 ±0.47
4	0.303	±0.017	1991.59 ±1.03	0.259	±0.008	1990.23 ±0.64	0.343	±0.011	1991.36 ±0.62
5	0.216	±0.009	1986.96 ±0.97	0.235	±0.008	1985.98 ±0.79	0.125	±0.004	1983.33 ±0.91
6	0.145	±0.006	1980.07 ±1.25	0.284	±0.010	1982.46 ±0.96	0.111	±0.004	1974.31 ±1.13
7	0.491	±0.058	1978.04 ±3.75	0.214	±0.007	1977.78 ±1.09	0.268	±0.009	1970.57 ±1.27
8	0.225	±0.015	1973.60 ±2.42	0.228	±0.008	1973.39 ±1.36	0.207	±0.006	1965.73 ±1.21
9	0.244	±0.020	1969.50 ±3.39	0.199	±0.007	1968.37 ±1.49	0.139	±0.005	1958.52 ±1.75
10	0.202	±0.017	1964.56 ±3.80	0.178	±0.006	1962.76 ±1.72	0.126	±0.006	1950.59 ±2.81
11	0.159	±0.009	1958.25 ±2.83	0.176	±0.006	1957.08 ±1.93	0.080	±0.004	1938.04 ±3.87
12	0.120	±0.007	1949.94 ±3.49	0.133	±0.005	1949.54 ±2.23	0.031	±0.001	1905.66 ±4.49
13	0.126	±0.008	1941.98 ±4.60	0.190	±0.007	1944.28 ±2.53	0.016	±0.001	1842.28 ±7.28
14	0.111	±0.008	1932.97 ±5.48	0.272	±0.011	1940.60 ±2.87	0.033	±0.002	1812.40 ±9.16
15	0.069	±0.007	1919.43 ±9.11	0.099	±0.004	1930.53 ±3.29			
16	4.123	±1.458	1919.01 ±3.29	0.182	±0.008	1925.04 ±3.79			
17	1.999	±0.626	1918.17 ±8.76	0.241	±0.010	1920.89 ±3.77			
18	0.036	±0.002	1890.55 ±7.75	0.078	±0.003	1908.07 ±4.18			
19	0.042	±0.005	1866.53 ±16.93	0.098	±0.004	1897.90 ±4.78			
20				2.606	±0.120	1897.52 ±5.19			
21				0.275	±0.012	1893.88 ±5.19			
22				0.039	±0.002	1868.25 ±6.15			
23				0.186	±0.008	1862.88 ±6.62			

did not display exponential decrease with depth in eastern Lake Superior.

In this study porosities have not displayed the exponential decreases along to sediment profiles. Porosity varies between 0.82 and 0.77 from top to bottom levels in central area of the lake and between 0.70 and 0.68 from top to bottom levels in near shore. When glimpsed to the Fig. 2, it can be seen that the sediments accumulated to the lake floor are homogenous in C-1 and C-3 stations separately.

Since the porosity is consistent at layer by layer along to core profile. In C-2 station first part which is long 23 cm of the core, displays the fluctuations on porosity so it can be said that C-2 has a stratified construction.

Radionuclides

The relation between ²¹⁰Po concentrations and porosities along to the core profiles can be seen that, however profile

Table 3 Sedimentation rates and dating in cores C-1, C-3, C-4 using CRS model

Depth (cm)	C-1				C-3				C-4			
	SR (cm year ⁻¹)		Dating (year)		SR (cm year ⁻¹)		Dating (year)		SR (cm year ⁻¹)		Dating (year)	
1	0.19	±0.008	2004.73	±0.21	0.202	±0.005	2005.06	±0.13	0.107	±0.003	2000.7	±0.28
2	0.237	±0.010	2000.52	±0.39	0.199	±0.006	2000.04	±0.28	0.181	±0.006	1995.19	±0.49
3	0.185	±0.006	1995.13	±0.52	0.17	±0.005	1994.16	±0.43	0.231	±0.007	1990.85	±0.57
4	0.309	±0.017	1991.89	±1.01	0.265	±0.009	1990.38	±0.64	0.334	±0.011	1987.86	±0.73
5	0.208	±0.009	1987.09	±0.97	0.238	±0.008	1986.18	±0.78	0.124	±0.004	1979.78	±1.03
6	0.148	±0.006	1980.32	±1.24	0.28	±0.010	1982.6	±0.96	0.111	±0.004	1970.79	±1.24
7	0.49	±0.058	1978.28	±3.73	0.212	±0.007	1977.9	±1.09	0.275	±0.009	1967.15	±1.38
8	0.227	±0.015	1973.87	±2.40	0.226	±0.008	1973.47	±1.36	0.208	±0.006	1962.35	±1.30
9	0.249	±0.021	1969.86	±3.36	0.197	±0.007	1968.4	±1.49	0.138	±0.005	1955.11	±1.86
10	0.203	±0.017	1964.92	±3.77	0.178	±0.006	1962.79	±1.72	0.124	±0.006	1947.06	±2.98
11	0.157	±0.009	1958.54	±2.81	0.171	±0.006	1956.93	±1.94	0.078	±0.004	1934.24	±4.07
12	0.12	±0.007	1950.21	±3.48	0.132	±0.005	1949.34	±2.23	0.031	±0.001	1902.2	±4.64
13	0.127	±0.009	1942.33	±4.57	0.192	±0.007	1944.15	±2.54	0.016	±0.001	1839.99	±7.38
14	0.111	±0.008	1933.32	±5.45	0.271	±0.011	1940.45	±2.88	0.033	±0.002	1810.12	±9.27
15	0.069	±0.007	1918.78	±9.07	0.1	±0.004	1930.42	±3.29				
16	4.169	±1.474	1919.02	±32.16	0.181	±0.008	1924.91	±3.80				
17	2.021	±0.633	1918.52	±28.65	0.242	±0.010	1920.77	±3.77				
18	0.036	±0.002	1890.91	±7.73	0.079	±0.003	1908.18	±4.17				
19	0.041	±0.005	1866.53	±16.93	0.1	±0.004	1898.15	±4.77				
20					2.573	±0.119	1897.76	±5.18				
21					0.274	±0.012	1894.11	±5.18				
22					0.039	±0.002	1868.34	±6.15				
23					0.185	±0.008	1862.93	±6.61				

distributions of ²¹⁰Po displayed the exponential decrease with increasing depth (Table 1), in C-1 and C-3 stations porosity shows more or less constant line from top to bottom along to the profiles on the Fig. 2. In other cores (C-2 and C-4) profile distribution of ²¹⁰Po concentrations do not display exponential decrease with increasing depth and porosity showed sequentially increases and decreases along to the core profile. So we think that exponential decrease in porosity for exponential decrease with increasing depth in ²¹⁰Po concentrations conversely to Begy et al. [10] is not necessary.

²¹⁰Po/²¹⁰Pb ratios in sediment cores provide the important information which is related to the sediment nature. According to Boisson et al. [12] the ratio is generally close to 1 in sediments, approximately 2 in fecal pellets (fecal pollution or dead plankton), 7 in phytoplankton and 30 in zooplankton detrital material. Further information about the ²¹⁰Po/²¹⁰Pb ratios in surficial waters can be found in Masque et al. [13]. The ranges of ratios in the sediment cores obtained from the Lake Bafa were 2.27–1.32, 1.52–0.90, 2.78–0.79, 1.84–0.76 in C-4, C-3, C-2, C-1 stations respectively (Table 1). They indicate that nature of the precipitated particles to the lake floor is close to fecal pellets

especially in C-4 station in Lake Bafa. Heussner et al. [14] and Wei and Murray [15] were reported that the average ratio in particles were 0.68–1.13 for North-western Mediterranean and the Black Sea. Average ²¹⁰Po/²¹⁰Pb ratios in C-3, C-2 and C-1 (0.96, 1.15, and 1.13 respectively) stations are more or less at same interval with North-western Mediterranean and Black Sea. However, in C-4 (1.58) station it is higher than the above ratio.

Some radionuclides like ²¹⁰Pb and ¹³⁷Cs have been used in environmental studies. ²¹⁰Pb is the important natural radionuclide for determining marine and fresh water sedimentation and it provides well-established mathematical models [16–21]. These models have been extensively used in dating the chemical changes, trace or heavy metal, organic matter and any other kind of pollution that have occurred in recent lake sediments [22–24]. Application of radiometric methods to sedimentary geochronology resulted successfully. According to the Krishnaswami et al. [25] ²¹⁰Pb is ideal for dating lake sediments as far back as a century or so [26].

The ²¹⁰Pb dating is generally supported by the marker ¹³⁷Cs since the use of both radiotracers improves accuracy by providing two independent means of measuring the

same burial processes occurring within a given sediment core. The artificial radionuclide ^{137}Cs aroused from the atmospheric testing of thermo nuclear weapons and Chernobyl reactor accident then precipitated to environment. Significant fallout on a global scale began after the initial test in the early 1950s, reached peak value in 1963 and then declined because of the implementation of the international treaty banning such tests. Next nuclear weapons tests in the atmosphere between 1966 and 1974 were performed by France. Other substantial fallout originated with 1986 Chernobyl Reactor Accident.

Although ^{210}Pb can be determined by alpha (via indirectly its grand-daughter, ^{210}Po), beta (via its beta emitting daughter, ^{210}Bi (half-life: 5.01 days)) or gamma spectrometric methods ^{210}Po analysis is widely realized using alpha spectrometric methods [27, 28]. So in this study ^{210}Pb and ^{137}Cs were determined by alpha and gamma spectrometric methods respectively.

The total ^{210}Pb activity in sediments has two components, namely supported and unsupported components. Unsupported ^{210}Pb is that part of the measured activity of the ^{210}Pb which exceeds the supported activity that derives from in situ decay of the parent radionuclide ^{226}Ra and it will usually be in radioactive equilibrium with the ^{226}Ra . Unsupported ^{210}Pb is determined by subtracting supported activity from the total activity at every levels. ^{210}Pb is scavenged from the atmosphere by both wet and dry processes as ^{210}Po [29–32].

The total ^{210}Pb activity is varied between $170.74 \pm 4.78 \text{ mBq g}^{-1}$ and $54.80 \pm 2.57 \text{ mBq g}^{-1}$ along the core in C-1 station. ^{226}Ra activity was determined as $54.80 \pm 2.57 \text{ mBq g}^{-1}$ from the deepest layer of the core (the layer is defined that the total ^{210}Pb activity decreases to level of ^{226}Ra activity as deepest layer in dating and remained part of the core is ignored.). Unsupported ^{210}Pb activities were plotted on logarithmic scale versus depth profile and slope of the graph was 0.237 (Fig. 3.). Inclination of the graph was determined by the regression line ($r^2 = 0.884$). This line is sufficiently fit for logarithmic ^{210}Pb concentrations in core C-1. So in calculation of sedimentation rates all models (CRS, CIC and CF;CS) are more or less compatible with each other. Sedimentation rate which is calculated by the CF;CS model is $0.131 \text{ cm year}^{-1}$ but CIC and CRS models are useable rather than CF;CS. Beside of the ^{210}Pb dating models, ^{137}Cs method utilized to confirm the sedimentation rates or sediment dating in C-1 station. The most suitable model is the CIC in this core. Since the results of the ^{210}Pb dating (CIC model) are a bit more compatible with the results of the ^{137}Cs dating than the other one (CRS model). When it is glanced to the ^{137}Cs activities Chernobyl and nuclear test peaks are seen in Fig. 4. ^{137}Cs activities reached to a peak value ($50.00 \pm 2.78 \text{ mBq g}^{-1}$) at the fifth cm under the sediment surface in core C-1

(Fig. 4.). It indicates that fifth cm under the sediment surface corresponds to the 1986 (Chernobyl reactor accident). As it can be clearly seen from Tables 2 and 3. It is necessary 23.04 ± 0.97 years and 22.91 ± 0.97 years according to CIC and CRS models respectively for sediment deposition from surface to fifth cm under the sediment surface. Second peak ($10.17 \pm 1.37 \text{ mBq g}^{-1}$) is seen at the twelfth cm under the surface. This peak belongs to the nuclear test attempts. It corresponds to 59.79 ± 3.48 and 60.06 ± 3.49 years before according to CRS and CIC models respectively (Tables 3 and 2). It can be seen that the each sediment dating techniques, natural radionuclide ^{210}Pb (CIC and CRS models) and artificial radionuclide ^{137}Cs have shown good agreement in this station.

Sedimentation rate is varied between $1.999 \pm 0.626 \text{ cm year}^{-1}$ and $0.036 \pm 0.002 \text{ cm year}^{-1}$ along to core. ^{210}Pb flux ($21.24 \text{ mBq cm}^{-2} \text{ year}^{-1}$) was calculated by using core inventory ($683.34 \text{ mBq cm}^{-2}$). Although sedimentation rate displays the successive increases and decreases, in general it increases until the seventh layer ($0.491 \pm 0.058 \text{ cm year}^{-1}$) than decreases through to the deeper parts of the core except seventeenth layer ($1.999 \text{ cm year}^{-1}$). Sediment deposition has displayed the increasing inclination until 1969 and it has showed successive fluctuations at last thirty years. The reasons of the fluctuations on sediment deposition may be related to the growing agricultural areas and changing irrigation policy around the lake. According to Persson and Holm [33] phosphate fertilizers are derived from phosphate ores containing ^{210}Pb and ^{210}Po [34, 35]. Most of the contaminants are left in the solid gypsum waste, and some of the ^{210}Pb and ^{210}Po and in the fertilizers [36, 37]. Disposing gypsum waste directly into the environment and the use of phosphate fertilizers may affect the levels of ^{210}Pb and ^{210}Po in water sediments and soil [36, 38–40]. The phosphate industry is claimed to be a major source of enhancement of ^{210}Pb and ^{210}Po in the surrounding environment [41].

Distribution of the total ^{210}Pb activity is varied between $44.81 \pm 2.63 \text{ mBq g}^{-1}$ and $42.12 \pm 2.84 \text{ mBq g}^{-1}$ along the core in C-2 station. Vertical distribution of ^{210}Pb activity along to core is not display the exponential decrease so dating or sedimentation rate cannot be calculated in this station. According to us overlapping sediment layers have collapsed and sediment layers have mixed each other. Average $^{210}\text{Po}/^{210}\text{Pb}$ ratio (1.15) displays the sediment type. Accumulated sediment is not comprised the soft material. In this case collapsing of the sediment layers may be related to the geologic features of the lake floor. For instance, an earthquake may have triggered the collapse of the sediment layers accumulated on sloping lake floor.

The total ^{210}Pb activity is varied between $187.84 \pm 4.83 \text{ mBq g}^{-1}$ and $58.46 \pm 2.56 \text{ mBq g}^{-1}$ along the core in C-3 station. ^{137}Cs activity concentrations gave the

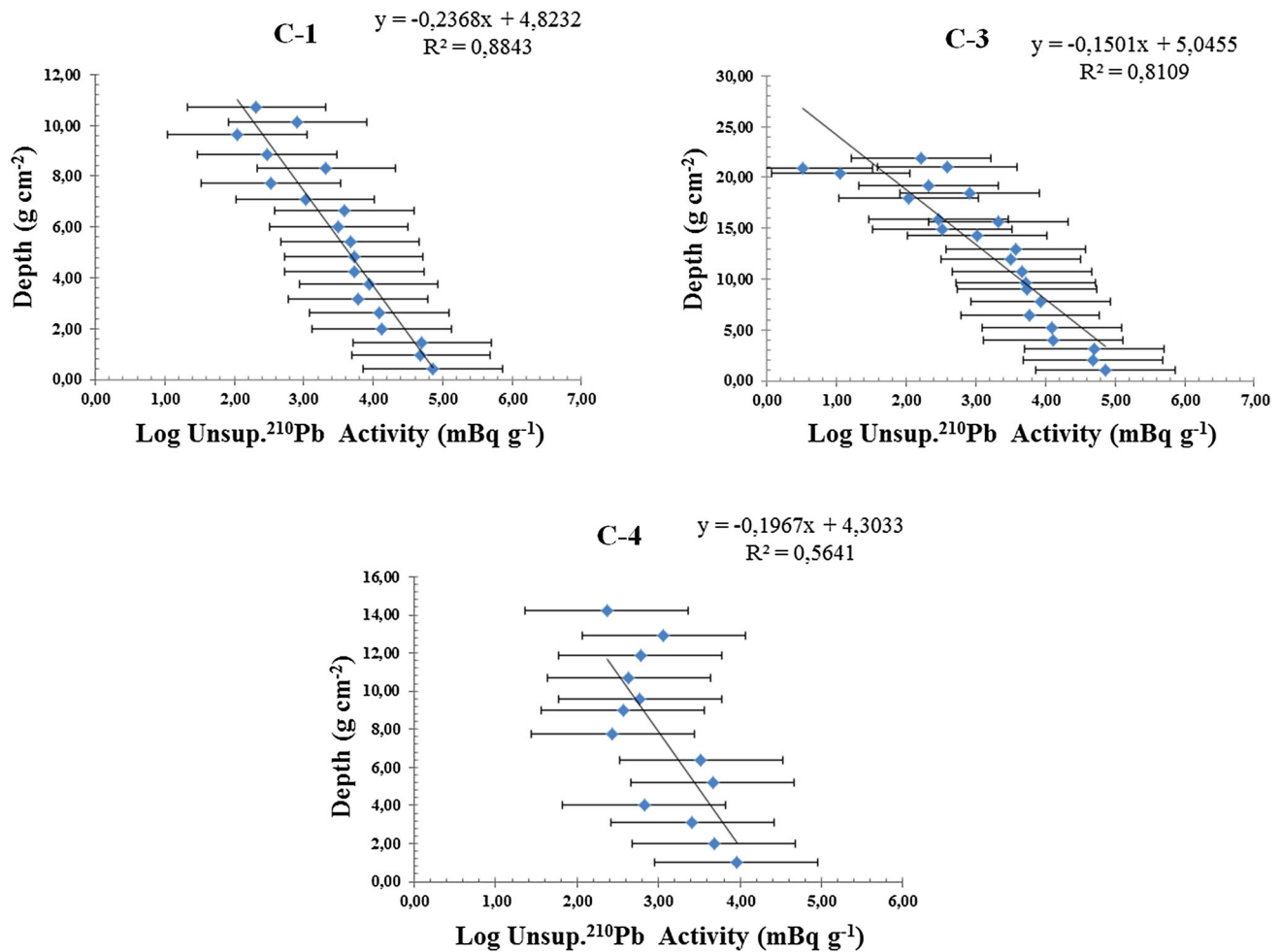


Fig. 3 Unsupported ^{210}Pb concentrations were plotted on logarithmic scale versus mass depth in Lake Bafa cores (C-1, C-3 and C-4). Slope of the regression line and regression coefficient were indicated upper right-hand corner in each graph

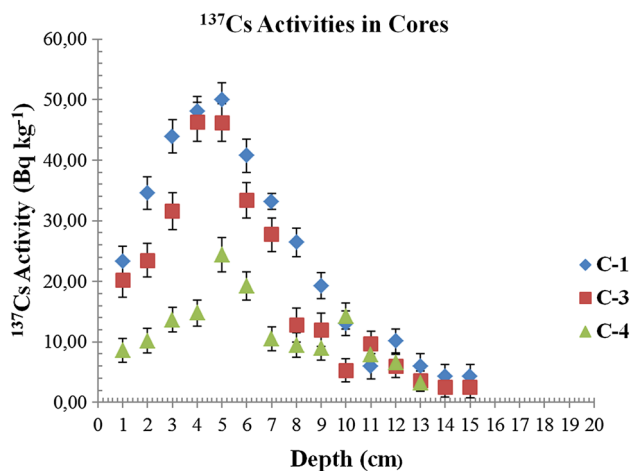


Fig. 4 Profile distribution of ^{137}Cs activity concentrations in C-1, C-3 and C-4 cores

Chernobyl and nuclear test peak. ^{137}Cs concentrations reached to a peak value ($46.32 \pm 3.25 \text{ mBq g}^{-1}$) at the fifth cm under the sediment surface in core C-3 (Fig. 4.). It is indicated that fifth cm under the sediment surface corresponds to the 1986 (Chernobyl reactor accident). As it can be clearly seen from Tables 2 and 3. It is necessary 24.02 ± 0.79 years and 23.82 ± 0.78 years according to CIC and CRS models respectively for sediment deposition from surface to fifth cm under the sediment surface. The next peak ($9.67 \pm 1.63 \text{ mBq g}^{-1}$) which is belong to nuclear test attempts (1957), is at eleventh cm under the surface. It corresponds to 63.07 ± 1.94 and 62.92 ± 1.93 years before according to CRS and CIC models respectively. If error range (Tables 2 and 3) is considered it is very close to beginning of the first nuclear test reaction (1951) or to 1963 peak (late 1950s/early 1960s).

Sedimentation rate is varied between 2.606 ± 0.120 and 0.039 ± 0.002 cm year⁻¹ along to core. ²¹⁰Pb flux (27.72 mBq cm⁻² year⁻¹) was calculated by using core inventory (892.09 mBq cm⁻²).

Distribution of the total ²¹⁰Pb activity ranged between 126.34 ± 3.42 mBq g⁻¹ and 74.25 ± 2.66 mBq g⁻¹ along the core in C-4 station. When it is glanced to the ¹³⁷Cs activities, Chernobyl and nuclear test peaks are seen obviously. ¹³⁷Cs activities reach to a peak value (24.35 ± 1.28 mBq g⁻¹) at the fifth cm under the sediment surface in core C-4 (Fig. 4). According to the CIC model fifth cm under the sediment surface corresponds to the 1983. If error range (Table 2) is considered it is very close to the 1986 (Chernobyl reactor accident). Second peak is seen at tenth cm (13.09 ± 1.03 mBq g⁻¹) under the sediment surface corresponds to beginning of the first nuclear test reactions (1951). It can be clearly seen from Table 2. It is necessary 59.41 ± 2.81 years according to CIC model for sediment deposition from surface to tenth cm under the sediment surface. It can be seen that the each sediment dating techniques natural radionuclide ²¹⁰Pb (CIC and CRS models) and artificial radionuclide ¹³⁷Cs have shown good agreement in this station. Small differences may be related to the sediment structure or particle reactive feature of the ¹³⁷Cs. Sediment structure is close to fecal pellets as different from the other stations. Water depth is 3 m in this station. Direction of the wind has affected the accumulated materials such as peat and algae for C-4 station. Because algae are comprised on the surface of lake water and they are moved to C-4 station by wind. Sedimentation rate is varied between 0.343 ± 0.011 and 0.016 ± 0.001 cm year⁻¹ along to core. ²¹⁰Pb flux (10.22 mBq cm⁻² year⁻¹) is calculated by using core inventory (328.82 mBq cm⁻²).

Max. unsupported ²¹⁰Pb activities in Lake Bafa are slightly higher than those in Lake Puyehue and Lake Icalma (80 – 120 Bq kg⁻¹ and 90 Bq kg⁻¹ respectively) [42], Red Lake (Romania) (137.34 Bq kg⁻¹) [10], more or less same with Lough Carra (Ireland) (200 Bq kg⁻¹) [43] and lower than Lake Hongfeng (248 – 371 Bq kg⁻¹) [23].

Although inventories are different in each core, central ones (C-1, C-3) are close to each other and higher than the near shore one (C-4). Difference might be aroused from beside of the maximum core depths (short cores have lower ²¹⁰Pb inventory than the deeper one) sediment types. It is familiar that sediment type is directly related to the radionuclide absorbance. It is stated by Persson and Holm [33] that, soil consists of particles of different minerals as well as organic matter in various stages of degradation.

The ²¹⁰Pb fluxes (21.24 , 27.72 , 10.22 mBq cm⁻² year⁻¹) in Lake Bafa are higher than the ones at Northern Patagonia Lakes (it ranged from 4 to 48 Bq m⁻² year⁻¹) [20], and lower than Lake Zurich; Center of lake 3 (375 ± 38 Bq m⁻² year⁻¹) [44] (obtained from Guevara et al. [20]). According

to Appleby and Oldfield [18] global average atmospheric flux was estimated as 185 Bq m⁻² year⁻¹. Therefore we can say that average ²¹⁰Pb flux ($19,73$ mBq cm⁻² year⁻¹) obtained from Lake Bafa is a bit higher than the global average. However it is more or less in the range of average atmospheric flux values of the Mediterranean area that was reported by Garcia-Orellana et al. [45]. It is a bit lower than average ($204,30$ Bq m⁻² year⁻¹) atmospheric flux of Monaco [46].

In general, sedimentation rates along to core profile are more or less same in central cores (C-1 and C-3). They exhibited a stable character. According to us differences arise from the maximum core depths and the distributions of ²¹⁰Pb concentration along to core profiles. Since measured bottom currents are almost same in central stations of the lake and not sufficient for an impression on the sedimentation pattern. However sedimentation rates along to core profile are not systematic in C-4 station. Two different trends are seen in C-4 core. First, sedimentation rates show sharp increase and decrease between 1966 and 2010. Second, it is decreased from 1966 to 1813. Average sedimentation rate in central area cores are slightly higher than the near shore one. The sedimentation rates in more recent times are two and three times higher than the earlier years. The increasing inclination of the sedimentation rate among the sediment layers in near shore is higher than the central area of the lake. According to us, it should be related to the sediment types of stations and the prevailing winds. Since the usual wind direction for the lake is towards to C-4 station. Beside of this in hydrothermal areas sedimentation rates in upper layers are up to seven times higher than the bottom ones [47]. So we can say that Lake Bafa has not hydrothermal activity.

In entire study site mean atmospheric flux (24.48 mBq cm⁻² year⁻¹) in central area and near shore (10.22 mBq cm⁻² year⁻¹) are not close to each other. So it is indicated that the atmospheric flux is not the dominant factor controlling the ²¹⁰Pb supply. In this situation CIC model should be utilized for sediment dating [16–18, 48]. These models are compatible but CIC model also is displayed better convenience with ¹³⁷Cs method in general. In another research conducted by Müllenhoff et al. [2] two sediment cores were obtained from the lake. The first one (Baf S1) was taken from the eastern part of the lake, the second one (Baf S6) from the Midwestern part. Both cores have been analyzed with sedimentological, micro-faunistic and paly-nological methods. Dating has been realized by using radiocarbon technique (AMS-technique) in both cores. Their results are indicated that sedimentation rate increases from 0.11 cm year⁻¹ (11 cm/100a) in the Geometric-Archaic periods (Baf S1) and 0.22 cm year⁻¹ (22 cm/100a) in the Classical-Hellenistic periods (Baf S6), respectively, to 1.35 cm year⁻¹ (135 cm/100a) in the

Roman era. However in our study average sedimentation rate is found as $0.351 \text{ cm year}^{-1}$ in central area and $0.137 \text{ cm year}^{-1}$ in near shore station by using together ^{210}Pb and ^{137}Cs techniques.

Other knowledge about Lake Bafa is residence time of ^{210}Pb in lake water. According to Kumar et al. [8] in a lake sediment core, lower values of ^{210}Pb concentration at the sediment–water interface compared to values at lower depths and/or a non-monotonic ^{210}Pb profile at any location beside of the other things may be attributable to higher residence time of the radionuclide in lake water. It was calculated by using profile distribution of ^{210}Pb concentrations as 1.9 months for Lake Bafa. The residence time of ^{210}Pb in Lake Bafa waters is very short. So it is convenient with non-lower values of ^{210}Pb concentration at the sediment–water interface in lake. According to us it is next indicator to explain sedimentation pattern and accumulated sediment type.

Conclusions

The study has focused on to answering the question “How to describe recent changes on Lake Bafa using especially radiometric techniques?” In order to response the question, sediment porosities were calculated, radionuclide concentrations were determined, bottom currents were measured, and residence time of ^{210}Pb was calculated in lake water. The results showed that sediment structure had a stratified construction in C-2 and homogenous one in C-1 and C-3 along to cores. The evaluation of relation between porosities and ^{210}Po concentrations in cores indicated that exponential decrease with increasing depth was not an obligation on porosity and ^{210}Po concentrations in a parallel manner. The other important information was received from radionuclide ($^{210}\text{Po}/^{210}\text{Pb}$) ratios in sediment cores. The range of ratios could be said that nature of the precipitated particles to the lake floor as sediment is close to fecal pellets (fecal pollution). It may be related to the buildings around the lake or salinity difference of the lake water between in summer and winter seasons. Because entry of waters that are coming from Menderes River to lake has been blocked for irrigation in summer months, in recent years. A hydraulic barrier controlling the lake’s water level with two regulators at both ends have been installed. So salinity difference has caused uncontrolled reproduction of alga on the water surface and than dead algae have sunk towards to bottom as sediment. It has been also supported by radiometric techniques ($^{210}\text{Po}/^{210}\text{Pb}$ ratio). It should be taken some protective measure related to the fecal pollution around the lake. In this study the sedimentation rates and sedimentation pattern of Lake Bafa were studied using natural ^{210}Pb models and tested by

utilizing ^{137}Cs technique. Sedimentation rates were evaluated with respected to bottom currents, porosities, profile distribution of ^{210}Pb concentrations, relations between $^{210}\text{Po}/^{210}\text{Pb}$ and sediment types, prevailing winds. Average sedimentation rate in central area of the lake was higher than the near shore region. According to us residence time of ^{210}Pb in lake water was next indicator to explain sedimentation pattern and accumulated sediment type. It was very short (1.9 months). So it was convenient with non-lower values of ^{210}Pb concentration at the sediment–water interface in lake. Sedimentation pattern was also evaluated with respect to the bottom currents. It was pointed out that speed of the bottom currents was very low and it was not sufficient to make any impression on sediment accumulation. Differences of the sedimentation rates among to stations were free from the bottom currents. So it can be said that the lake has different sediment depositional zones.

Although there is a study related to the sediment dating using radiocarbon technique. Due to the lack of available data about detailed sediment dating in Lake Bafa, we performed this detailed recent sediment dating of the lake. We provided the different point of view to Lake Bafa via using radiometric techniques. We think that the present study will provide to available and comparable data for next studies on this subject.

Acknowledgments This research work was supported by the Scientific and Technical Research Council of Turkish (TUBITAK) Contract ID: 110Y002.

References

1. Erdogan S (2011) A chemical reaction to a physical impact: Lake Bafa wetland ecosystem (Turkey) case. *Ankara Universitesi Cevrebilimleri Dergisi* 3(1):1–8
2. Müllenhoff M, Handl M, Knipping M, Brückner H (2004) The evolution of Lake Bafa (Western Turkey)-Sedimentological, microfaunal and palynological results. *Coastline Rep* 1:55–66
3. Ozel E, Yasar D, Eftelioglu M, Gunay C, Sert I (2011) Bafa Gölü’nün Jeolojisi—Jeofiziği ve Oşinografisinin Araştırılması Projesi Sonuç Raporu. Tübitak İzmir (in Turkish)
4. Flynn WW (1968) The determination of low levels of Polonium-210 in environmental materials. *Anal Chim Acta* 43:221–227
5. Bateman H (1910) Solution of a system of differential equations occurring in the theory of radioactive transformations. *Proceedings of the Cambridge Philosophical Society*, 15: 423–427
6. Cetnar J (2006) General solution of Bateman equations for nuclear transmutations. *Ann Nucl Energy* 33:640–645
7. Karadeniz O, Yaprak G (2007) Dynamic equilibrium of radiocesium with stable cesium within the soil-mushroom system in Turkish pine forest. *Environ Pollut* 148:316–324
8. Kumar US, Navada SV, Rao SM, Nachiappan RP, Kumar B, Krishnamoorthy TM, Jha SK, Shukla VK (1999) Determination of recent sedimentation rates and pattern in Lake Naini, India by ^{210}Pb and ^{137}Cs dating techniques. *Appl Radiat Isot* 51:97–105
9. Athy LF (1930) Density, porosity and compaction of sedimentary rocks. *Bull Am Assoc Petrol Geol* 14:1–24

10. Begy R, Cosma C, Timar A (2009) Recent changes in Red Lake (Romania) sedimentation rate determined from depth profiles of ^{210}Pb and ^{137}Cs radioisotopes. *J Environ Radioact* 100:644–648
11. Klump JV, Paddock R, Remsen CC, Fitzgerald S, Boraas M, Anderson P (1989) Variations in sediment accumulation rates and the flux of labile organic matter in Eastern Lake Superior Basin. *J Great Lakes Res* 15(1):104–122
12. Boisson F, Miquel JC, Cotret O, Fowler SW (2001) ^{210}Po and ^{210}Pb cycling in an hydrothermal vent zone in the coastal Aegean Sea. *Sci Total Environ* 281:111–119
13. Masque P, Sanches-Cabeza JA, Bruach JM, Palacios E, Canals M (2002) Balance and residence times of ^{210}Pb and ^{210}Po in surface waters of the Northwestern Mediterranean Sea. *Cont Shelf Res* 22:2127–2146
14. Heussner S, Cherry R, Heyraud M (1990) ^{210}Po and ^{210}Pb in sediment trap particles on a Mediterranean continental margin. *Cont Shelf Res* 10(9–11):989–1004
15. Wei CL, Murray JW (1994) The behavior of scavenged isotopes in marine anoxic environments: ^{210}Pb and ^{210}Po in the water column of the Black Sea. *Geochim Cosmochim Acta* 58:1795–1811
16. Appleby PG (2001) Chronostratigraphic techniques in recent sediments. In: Last WM, Smol JP (eds) *Tracking environmental change using Lake sediments*, vol 1. Springer, Dordrecht, pp 171–203
17. Appleby PG, Oldfield F (1978) The calculation of lead-210 dates assuming a constant rate of supply of unsupported ^{210}Pb to the sediment. *Catena* 5:1–8
18. Appleby PG, Oldfield F (1983) The assessment of ^{210}Pb data from sites with varying sediment accumulation rates. *Hydrobiologia* 103:29–35
19. Gelen A, Soto J, Gómez J, Díaz O (2004) Sediment dating of Santander Bay, Spain. *J Radioanal Nucl Chem Lett* 261(2):437–441
20. Guevara SR, Rizzo A, Sánchez R, Arribére M (2003) ^{210}Pb fluxes in sediment layers sampled from northern Patagonia lakes. *J Radioanal Nucl Chem Lett* 258(3):583–595
21. McDonald CP, Urban NR (2007) Sediment radioisotope dating across a stratigraphic discontinuity in a mining-impacted lake. *J Environ Radioact* 92:80–95
22. Evenset A, Christensen GN, Carroll J, Zaborska A, Berger U, Herske D, Gregor D (2007) Historical trends in persistent organic pollutants and metals recorded in sediments from Lake Ellasjøen, Bjornoya, Norwegian Arctic. *Environ Pollut* 146:196–205
23. Xu L, Wu F, Wan G, Liao H, Zhao X, Xing B (2011) Relationship between $^{210}\text{Pb}_{\text{ex}}$ activity and sedimentary organic carbon in sediments of 3 Chinese Lakes. *Environ Pollut* 159:3462–3467
24. Yuan G, Liu C, Chen L, Yang Z (2011) Inputting history of heavy metals into the inland lake recorded in sediment profiles: Poyang Lake in China. *J Hazard Waste Hazard* 185:336–345
25. Krishnaswami LD, Martin JM, Meybeck M (1971) Geochronology of lake sediments. *Earth Planet Sci Lett* 11:407–414
26. Robbins JA, Edgington DN (1975) Determination of recent sedimentation rates in Lake Michigan using Pb-210 and Cs-137. *Geochim Cosmochim Acta* 39:285–304
27. Baskaran M (2011) Po-210 and Pb-210 as atmospheric tracers and global atmospheric Pb-210 fallout: a review. *J Environ Radioact* 102:500–513
28. Villa M, Hurtado S, Manjón G, Gacía-Tenorio R (2007) Calibration and measurement of ^{210}Pb using two independent techniques. *Radiat Meas* 42:1552–1560
29. Qi S, Leippe T, Rueckert P, Di Z (2010) Geochemical sources, deposition and enrichment of heavy metals in short sediment cores from the Pearl River Estuary, Southern China. *J Mar Systems* 82:28–42
30. Pfitzner J, Brunskill G, Zagorskis I (2004) ^{137}Cs and excess ^{210}Pb deposition patterns in estuarine and marine sediment in the central region of the Great Barrier Reef Lagoon, North-eastern Australia. *J Environ Radioact* 76:81–102
31. Turekian KK, Nozaki Y, Benninger LK (1977) Geochemistry of atmospheric radon and radon products. *Annu Rev Earth Planet Sci* 5:227–255
32. Bacon MP, Spencer DW, Brewer PG (1976) $^{210}\text{Pb}/^{226}\text{Ra}$ and $^{210}\text{Po}/^{210}\text{Pb}$ disequilibria in sea water and suspended particle matter. *Earth Planet Sci Lett* 32:277–296
33. Persson BRR, Holmb E (2011) International topical meeting on polonium and radioactive lead isotopes polonium-210 and lead-210 in the terrestrial environment: a historical review. *J Environ Radioact* 102(5):420–429
34. AlMasri MS, Mamish S, Budeir Y (2002) The impact of phosphate loading activities on near marine environment: the Syrian coast. *J Environ Radioact* 58:35–44
35. Othman I, Yassine T, Bhat I (1994) Measurements of some radionuclides in the marine coastal environment of Syria. *Sci Total Environ* 153:57–60
36. Aoun M, El Samrani AG, Lartiges BS, Kazpard V, Saad Z (2010) Releases of phosphate fertilizer industry in the surrounding environment: investigation on heavy metals and polonium-210 in soil. *J Environ Sci* 22:1387–1397
37. Rutherford PM, Dudas MJ, Samek RA (1994) Environmental impacts of phosphogypsum. *Sci Total Environ* 99:1–38
38. Barisic D, Lulic S, Milatic P (1992) Radium and uranium in phosphate fertilizers and their impact on the radioactivity of water. *Water Res* 26:607–611
39. Becker P (1985) Phosphates and phosphoric acids: raw materials in the Netherlands. *Sci Total Environ* 45:151–156
40. Carvalho FP (1995) Po210 and Pb210 intake by the Portuguese population – the contribution of seafood in the Dietary intake of Po210 and Pb210. *Health Phys* 69:469–480
41. Jimenez F, Lopez R, Deban L, Pardo R, GarciaTalavera M (2007) Po-210 and major ions in drainage water from soil treated with various types of fertilizers. *J Environ Sci Health Part A Toxic/Hazard Subst Environ Eng* 42:1051–1056
42. Arnaud F, Magand O, Chapron E, Bertrand E, Boës X, Charlet F, Mélières M-A (2006) Radionuclide dating (^{210}Pb , ^{137}Cs , ^{241}Am) of recent lake sediments in a highly active geodynamic setting (Lakes Puyehue and Icalma-Chilean Lake District). *Sci Total Environ* 366:837–850
43. O'Reilly J, Vintró LL, Mitchell PI, Donohue I, Leira M, Hobbs W, Irvine K (2011) ^{210}Pb -dating of a lake sediment core from Lough Carra (Co. Mayo, western Ireland): use of paleolimnological data for chronology validation below the ^{210}Pb dating horizon. *J Environ Radioact* 102:495–499
44. Von Gunten HR, Moser RN (1993) How reliable is the ^{210}Pb dating method? Old and new results from Switzerland. *J Paleolimnol* 9(2):161–178
45. Garcia-Orellana J, Sanchez-Cabeza JA, Masque P, Àvila A, Costa E, Loÿe-Pilot MD, Bruach-Menchén JM (2006) *J Geophys. Res.* doi:10.1029/2005JD006660
46. Pham MK, Povinec PP, Nies H, Betti M (2013) Dry and wet deposition of ^7Be , ^{210}Pb and ^{137}Cs in Monaco air during 1998–2010; Seasonal variations of deposition fluxes. *J Environ Radioact* 120:45–57
47. Sert I, Yener G, Ozel E, Pekcetinoz B, Eftelioglu M, Gorgun AU (2012) Estimation of sediment accumulation rates using naturally occurring ^{210}Pb models in Gulbahce Bay, Aegean Sea, Turkey. *J Environ Radioact* 107:1–12
48. Parsons MJ, Long DT, Yohn SS (2010) Assessing the natural recovery of a lake contaminated with Hg using estimated recovery rates determined by sediment chronologies. *Appl Geochem* 25:1676–1687